Enhancing Thermoelectric Efficiency Through Combined and Shunt Solar Chimneys: An Investigation of Vented Photovoltaic Panels with Multiple Inlets

Doubik Yemboate Lare[1], Yawovi Nougblega[1,2]*, Kodjo Kpode[3], Komi Apéléte Amou[2,4]

[1] Laboratoire Sur l'Energie Solaire, Groupe Phénomène de Transfert et Energétique, Université de Lomé, 01 Lomé BP 1515, Togo
[2] Regional Centre of Excellence on Electricity Management (CERME), University of Lomé, 01 Lomé BP 1515, Togo
[3] Laboratoire de Matériaux, Energie Renouvelable et Environnement, Université de Kara, Kara 404, Togo
[4] Laboratoire Sur l'Energie Solaire, Département de Physique, Faculté Des Sciences (FDS), Université de Lomé, 01 Lomé BP 1515, Togo

Corresponding Author Email: nycogl@yahoo.fr

ABSTRACT

This paper presents a computational analysis of the thermoelectric efficiency of hybrid solar chimneys equipped with ventilated photovoltaic (PV) panels with multiple fresh air inlets. The problem addressed is the overheating of the photovoltaic cells, which reduces their electrical efficiency. The influence of multiple air inlets on the electrical and thermal performance of PV/T collectors is the focus of this study. The main objective is to reduce the overheating of the photovoltaic cells and improve their efficiency. This is achieved by using multiple passive ventilation sources instead of placing ventilation systems behind the photovoltaic panels to extract heat and distribute warm air. The implicit finite difference approach is used to discretize the governing heat and mass transfer equations, which are then solved using the Thomas algorithm and the iterative Gauss-Seidel method. The results are obtained by adjusting several important factors, including Raleigh and Reynolds numbers and chimney geometric aspects. The results show that the simultaneous addition of several fresh air openings improves the thermal efficiency by 68% and the electrical efficiency by 5% compared to a chimney with a single vertical duct. The study concludes that this system offers an effective solution for improving the performance of photovoltaic panels, thus contributing to clean energy production.

1. INTRODUCTION

Increasing interest in renewable energy as fossil fuel resources depleted [1]. Research and development efforts have been made over the past few decades to find dependable and financially feasible substitute sources of clean energy. There are three types of energy: Geothermal, wind, and solar. Solar energy is the most abundant source of energy and is widely used for both heating and cooling applications [2]. The technique known as photovoltaic (PV) converts solar energy into electrical energy. However, photovoltaic cells have a limited conversion efficiency when the temperature rises and only react to part of the solar energy band. Due to the low efficiency and expensive nature of photovoltaic modules, the concept of a hybrid photovoltaic-thermal panel system has emerged. The PV/T system combines a solar thermal collector and a photovoltaic module. The main advantages of the PV/T system are that it simultaneously improves electrical energy production, eliminates excess heat from the photovoltaic panel, and minimizes space requirements. The energy from the sun is then converted into heat energy and stored in the water or the air as follows [3]. Three primary categories exist for PV/T collectors: air, water, and air/water. Thermally liquid

PV/T collectors can achieve increased electrical output and thermal efficiency due to the improved thermal conductivity of the heat transfer fluid. But they are more complicated and more expensive and can pose serious problems of freezing in colder conditions. Over the past few years, there has been much research into the many different types of liquid systems. To illustrate this, Etier et al. [4] have conducted experiments on a PV/T system using actively cooled aqueous systems. The results showed that the electrical power increased by 6.9% compared to the standard system. A three-dimensional computational model of a waterborne photovoltaic/thermal (PV/T) system designed to boost solar power generation performance in warm climates has been presented by Salameh et al. [5]. The study shows that reducing the temperature of solar panels through water conditioning can increase their power and thermic output. Improves overall energy efficiency by providing an efficient methodology for optimizing PV/T system performance in high-temperature environments. A numerical model of a waterborne photovoltaic-thermal (PVT) hybrid solar system has been developed by El Alami et al. [6], a collector with a numerical model of a waterborne photovoltaic-thermal (PVT) hybrid solar system has developed by El Alami et al. [6], a collector with a new type

of heat collector (PVT-C with duct box). The approach is to simulate the output of the system under various climatic and operational circumstances. The results show that, in terms of effectiveness, the PVT-C has an electrical efficacy of around 12.11%, a thermal efficacy of around 78.59%, and a total energy efficacy of around 90.7% for an irradiance of 103 W/m^2. However, the electrical power efficiency of the photovoltaic module is only 9.09%, which is 3% lower than that of PVT-C. Xu and Kleinstreuer [7] demonstrated that nano-fluid-based solar PV/T collectors are more advantageous for silicon solar cells than poly-junction solar cells because the overall energy conversion efficiency of the PV/T system is better than that of the conventional nano-fluid system. Sathyamurthy et al. [8] conducted an experimental study on the use of hybrid CNT/Al nanolayers in a photovoltaic-thermal (PV/T) system to improve the electrical conversion rate of photovoltaic cells. Using a helical tube collector to optimize heat flow, the thermal and electrical performance of photovoltaic panels with and without a cooling system has been compared.

The average power output increases by 7.15% with water and 8.2% with nanofluide, but only by 6.2% with an independent photovoltaic panel. Effective heat evacuation has increased energy production by 11.7% when using water and 21.4% when using hybrid nanofluids. In addition, the entire PV/T system is extremely efficient. In comparison with water, the entire efficiency of the PV/T system using hybrid nanofluids was also increased by 27.3%. To achieve an increase in the efficiency of the photovoltaic-thermal (PV/T) systems, a new collector cooling system using the nanofluids Al_2O_3, TiO_2, and CuO has been developed according to the research carried out by Aydın et al. [9]. Three mass concentrations of 0.2%, 0.4%, and 0.6% were used along with continuous loads to evaluate the performances, and the result showed a maximum increase in electrical power for the nanofluid Al_2O_3 of 1.467% to 0.2%, which is a 5.49% improvement over the previous results. The nanofluid itself showed the largest temperature drops, with an average thermal return of 49.59%. The mean cooling temperatures for water, TiO_2 water, Al_2O_3 water, CuO water, and water were 9.14°C, 11.64°C, and 13.28°C respectively for a 0.2% temperature drop. The research showed that a nanofluid concentration of 0.4% is optimal for maximizing system efficiency. PV/T systems based on air are also less efficient than those based on liquids. Because air conducts heat less well. On the other hand, air systems require less maintenance, are more affordable, and are less complicated. To increase the reliability of compressed air PV/T systems, several designs and changes in geometry have been investigated in the last decade [10]. A comparison between three different photovoltaic air collectors and PV systems was conducted in Algiers by Slimani et al. [11]. They found the double-holed collector to be the best performer, with an average daily energy efficiency of 74%. To assess the performance of a photovoltaic-thermal (PV/T) collector, Dunne et al. [12] studied the temperature distribution and the influence of air on the PV cell entry and exit temperatures. They highlighted the importance of air duct depth and velocity, aspects that have been little explored in the existing literature. Two different electricity generation systems are evaluated: A conventional PV configuration and an integrated PV/T configuration. A comparison study examines two different solar energy configurations: the archetypal photovoltaic (PV) configuration and a hybrid configuration. Thermal and electrical characteristics were exploited to create

efficiency equations, which were then confirmed by experimentation. Simulating with ducts shows an increase in power generation effectiveness of around 14%. While reducing daily variability, the photovoltaic system optimizes electrical performance. Deepening the duct reduces its ability to conduct electricity and heat, but the air moving through the channel improves its operation. The most effective results are achieved with a conduit depth of 0.01 m and an air speed of 2.5 m/s. Patil et al. [13] used computational fluid dynamics (CFD) simulation to study the effect of air circulation on the efficiency and operation of a photovoltaic-thermal (PV/T) system. The results show that with airflow rates ranging from 0.04 to 0.1 kg/s at an irradiance of 800 W/m², maximum temperatures of 48.8°C, 48.4°C, 47.3°C and 24.5°C are achieved for the top surface of the PV/T system, the bottom area and the air inlet and outlet points respectively at a flow rate of 0.01 kg/s. These results show that airflow is essential for the thermoregulation and energy efficiency of solar photovoltaic (PV/T) systems. Sardarabadi et al. [14] proposed a cutting-edge hybrid PV/air collector system in a follow-up study. This involved two inexpensive changes to the conventional collector type: extending the surface area on the air duct walls and hanging a thin, flat sheet from the duct's midway. The results showed that these changes were very efficient in increasing the heat energy extracted and significantly reducing the PV module temperature, which in turn increased the overall module efficiency. The researchers used validated numerical data to determine how the depth and length of the channel and the airflow rate affected the total performance of the hybrid PV/T air system. In Busan, Korea, Choi et al. investigated a novel monophases double-flow air channel PV/T collector with a heterogeneous cross-sectional rib attached to the backing of the solar module [15]. With a mass flow of 0.07698 kg/s, the most remarkable electrical and total thermal performances were reached, with 14.81% and 71.54% respectively. An air-based PV/T collector with a single channel integrated into a thin flat plate attached to the cooling fins was proposed and tested by Mojumder et al. [16]. The highest electrical and thermal efficiencies were found to be 14.03% and 56.19%, respectively, with four cooling fins, a mass flow rate of 0.14 kg/s, and 700 W/m^2 of solar radiation. Their integration into the walls of buildings will be more beneficial to the occupants, given the extensive research into photovoltaic-thermal collectors using different heat transfer fluids.

Badi and Laatar [17] propose a passive cooling system for photovoltaic panels using an inclined channel with adiabatic extensions to remove heat by natural convection. This process optimizes the efficiency and durability of PV panels in hot climates by improving airflow by 65% and reducing the maximum temperature by 11%. This system is particularly suitable for drylands, where water is limited and passive cooling is paramount. Building-integrated photovoltaic-thermal (BIPV/T) systems can be easily integrated into the building shell. They are simultaneously generators of electricity and heat. BIPV/T systems not only have the ability to actively capture solar radiation compared to the standard building envelope components, but also reduce the need for the heating and air-conditioning of the built space [18]. A hybrid solar wall system operating in ventilation mode is presented by Xu et al. [19], in heating and electricity generation in the cold season and in water flow configuration mode the rest of the year to provide hot water and electricity once. The results show that with a water temperature above

40°C in summer and an indoor temperature of 18.6°C in the cold season, the daily electricity production is 0.12 kWh with an efficiency of 7.6% in the heating season and 0.65 kWh with an efficiency of 12.5% in the cooling season. According to the simulation modeling, the system also achieves passive cooling in the cold season and efficient space heating in the hot season. Chen et al. [20] presented a two-story, energy-efficient, detached, prefabricated solar building in Quebec City with an open-circuit, air-cooled bioclimatic building system coupled to a ventilated cement floor. It was shown that a bioclimatic building system can reduce the thermal behaviour of solar cells and has the potential to support space heating. The influence of some air conditioning configurations on the thermal and electrical efficiency of a solar panel in a bioclimatic building system was investigated by Lukasik and Wajs [21]. A numerical model combining the SST k-ω turbulence, Discrete Ordinates radiation models, and a solar load module was developed using ANSYS Fluent software to predict the system performance under different inlet conditions and configurations. The results indicate that the optimum heat recovery, one-third of 330 W/m², is obtained from a channel having an inlet depth of about 25 mm, an airflow of 7.5 m³/h, and an incident solar irradiation of 900 W/m². The maximum experimental electrical efficiency was 5.76% at a duct spacing of 50 mm. The geometric configuration chosen gave the highest airflow (7.5 m³/h) at an irradiance of 600 W/m². Although optimizing the design of an air-conditioned photovoltaic solar thermal system can increase its thermal efficiency, the temperature at the outlet of the air duct is often high enough to overheat the solar cells and reduce the efficiency of the photoelectric conversion. From a limited bibliographic study, it is clear that a hybrid photovoltaic-thermal system has a ventilation mechanism on the underside for heat dissipation. A fan then pushes the hot air through connections in the ducts serving the living rooms and possibly a thermodynamic water heater. A roof outlet is available for the removal of excess heat. Photovoltaics is a technology that makes maximum use of captured solar energy. This system can use the heat generated under the panels, unlike conventional photovoltaic panels. The photovoltaic technology combines photovoltaic solar panels (facing the sun), which produce electricity like photovoltaic panels, with thermal solar panels, whose rear side includes a ventilation device to recover and then diffuse hot air inside the house or an air intake of a thermodynamic tank. Compared to a conventional installation, this ventilation increases the performance of the modules. However, the effectiveness of multiple openings in fresh air jets for ventilating the overheated rear surfaces of hybrid photovoltaic solar panels has not, to our knowledge, been investigated. This research aims to introduce an innovative ventilation technique based on multiple fresh air intakes to improve the heat dissipation behind the photovoltaic cells in PV/T systems. This study proposes the addition of multiple fresh air inlets to better dissipate heat and thus improve the thermal and electrical performance of solar panels, as opposed to conventional systems that use a single opening or passive ventilation systems. The interest of this research lies in the improvement of energy performance by optimizing the ventilation behind the photovoltaic panels through the use of hybrid solar chimneys with multiple fresh air inlets. This study proposes a solution to maximize energy production and minimize heat loss. The enhancement of hybrid photovoltaic collectors' performance can diminish the necessity for costly active

cooling systems while augmenting the amount of energy that can be harvested per solar panel area. The integration of solar chimneys and PV/T systems into buildings can facilitate the creation of energy-efficient structures, thereby addressing the increasing demand for intelligent and sustainable construction. This will help meet the growing demand for smart and sustainable buildings. The findings of this research are particularly pertinent to regions with high temperatures, where the efficiency of solar panels is reduced, yet greater energy consumption is required. In this paper, the authors put forth a numerical study of a vertically glazed PV/T system whose duct has multiple fresh air inlets in the area covered by absorbers. The objective of this study is to evaluate the impact of varying the configuration of fresh air inlet openings on the electrical and thermal performance of a PV/T air system, in comparison with a simple PV/T collector with a single vertical fresh air inlet duct. The present study comprises a numerical analysis of a mixed convection problem in a vertical photovoltaic-thermal hybrid chimney with multiple fresh air jet inlet openings and a constant heat flow for heating and ventilation. In this analysis, the airflow enters the chimney through internal openings and exits the chimney through an external opening.

2. MATHEMATICAL EXPRESSION

2.1 Physics model

This paper presents a study of the airflow in two distinct vertical solar chimney designs, with a particular focus on their potential integration into multi-story buildings. The solar chimney in question comprises three distinct levels of fresh air inlet openings. Chimney 2 comprises a shunt duct of width d2, which serves to channel the inlet opening of the fresh air jet into the main duct of width d1. The latter is dedicated to evacuating the heat accumulation above the solar cell level. The thermal and electrical efficiency of each solar chimney configuration is evaluated in comparison to a simple vertical chimney. These chimney designs are illustrated in Figure 1.
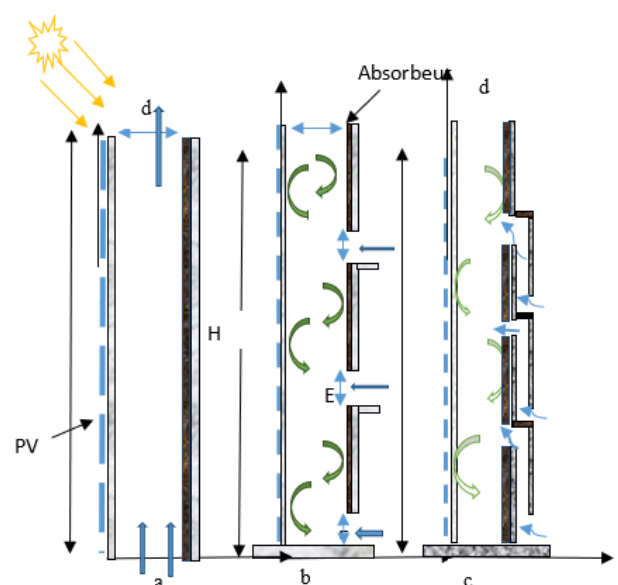

Figure 1. Diagram of the physical model
Solar chimney configurations: a) single chimney b) combination chimney c) shunt chimney

The principal heat transfer medium employed for the dissipation of surplus thermal energy from the solar cells is air. This investigation proposes a two-dimensional (2D) model of laminar mixed thermal convection in a transient state. The transfer equations are derived under the assumption that the air's temperature and thermophysical properties remain constant and that the fluid is perfectly incompressible and ideal. Furthermore, the Boussinesq approximation has been adopted.

2.2 Governing equations

Continuity equation

$$\frac{\partial U}{\partial X} + \frac{\partial V}{\partial Y} = 0 \tag{1}$$

Movement equation

$$\frac{\partial \Omega}{\partial \tau} + U\frac{\partial \Omega}{\partial X} + V\frac{\partial \Omega}{\partial Y} = \frac{1}{R_e}\left(\frac{\partial^2 \Omega}{\partial X^2} + \frac{\partial^2 \Omega}{\partial Y^2}\right) + R_i\frac{\partial \theta}{\partial X} \tag{2}$$

Energy equation

$$\frac{\partial \theta}{\partial \tau} + U\frac{\partial \theta}{\partial X} + V\frac{\partial \theta}{\partial Y} = \frac{1}{R_e P_r}\left(\frac{\partial^2 \theta}{\partial X^2} + \frac{\partial^2 \theta}{\partial Y^2}\right) \tag{3}$$

2.3 Associated boundary conditions

Initial conditions
At $\tau = 0$, $\theta = \Omega = \Psi = U = V = 0$
At $\tau > 0$
Combined chimney

$$X = 0; 0 < Y < D$$
$$U = V = 0; \Omega = -\frac{\partial^2 \Psi}{\partial X^2}\Big|_{X=0} \tag{4}$$
$$\frac{\partial \theta}{\partial X}\Big|_{X=0} = -(\tau_{gl}\alpha_{pv} - \eta_e)$$

$$X = 1; K < Y < D$$
$$U = V = 0; \Omega = -\frac{\partial^2 \Psi}{\partial X^2}\Big|_{X=1} \tag{5}$$
$$\frac{\partial \theta}{\partial X}\Big|_{X=1} = (\tau_{gl}\alpha_{abs}\alpha_{PV})$$

$$X = 1; 0 < Y < S$$
$$U = V = 0; \Omega = -\frac{\partial^2 \Psi}{\partial X^2}\Big|_{X=1} \tag{6}$$
$$\frac{\partial \theta}{\partial X}\Big|_{X=1} = (\tau_{gl}\alpha_{abs}\alpha_{PV})$$

$$X = 1; P < Y < A$$
$$U = V = 0; \Omega = -\frac{\partial^2 \Psi}{\partial X^2}\Big|_{X=1} \tag{7}$$
$$\frac{\partial \theta}{\partial X}\Big|_{X=1} = (\tau_{gl}\alpha_{abs}\alpha_{PV})$$

$$X = 1; A < Y < K$$
$$U = -1; V = 0; \Psi = -Y; \Omega = -\frac{\partial^2 \Psi}{\partial X^2}\Big|_{X=1} \tag{8}$$

$$\theta = 0$$
$$X = 1; 0 < Y < T$$
$$U = -1; V = 0; \Psi = -Y; \Omega = -\frac{\partial^2 \Psi}{\partial X^2}\Big|_{X=1}$$

$$\theta = 0$$
$$X = 1; S < Y < P \tag{9}$$
$$U = -1; V = 0; \Psi = -Y$$

$$\Omega = -\frac{\partial^2 \Psi}{\partial X^2}\Big|_{X=1}; \theta = 0 \tag{10}$$
$$Y = D; 0 < X < 1$$

$$\frac{\partial U}{\partial Y}\Big|_{Y=D} = 0; \frac{\partial V}{\partial Y}\Big|_{Y=D} = 0$$
$$\frac{\partial^2 \Psi}{\partial Y^2}\Big|_{Y=D} = 0; \frac{\partial \theta}{\partial Y}\Big|_{Y=D} = 0 \tag{11}$$

Shunt chimney

$$X = 0; 0 < Y < D$$
$$U = V = 0; \Omega = -\frac{\partial^2 \Psi}{\partial X^2}\Big|_{X=0} \tag{12}$$
$$\frac{\partial \theta}{\partial X}\Big|_{X=0} = -(\tau_{gl}\alpha_{pv} - \eta_e)$$

$$Y = 0; 0 < X < 1$$
$$U = V = 0; \Omega = -\frac{\partial^2 \Psi}{\partial Y^2}\Big|_{Y=0}; \frac{\partial^2 \Psi}{\partial Y^2}\Big|_{Y=0} = 0 \tag{13}$$
$$\frac{\partial \theta}{\partial Y}\Big|_{Y=0} = 0$$

Absorber plates

$$X = B$$
$$U = V = 0; \Omega = -\frac{\partial^2 \Psi}{\partial X^2}\Big|_{X=B}; \frac{\partial \theta}{\partial X}\Big|_{X=B} = (\tau_{gl}\alpha_{abs}\alpha_{PV}) \tag{14}$$

Inlet openings

$$X = 1$$
$$U = -1; V = 0; \Psi = -Y; \Omega = -\frac{\partial^2 \Psi}{\partial X^2}\Big|_{X=1}; \theta = 0 \tag{15}$$

$$U = \frac{\partial \Psi}{\partial X}; V = -\frac{\partial \Psi}{\partial Y}; \Omega = -\left(\frac{\partial^2 \Psi}{\partial X^2} + \frac{\partial^2 \Psi}{\partial Y^2}\right) \tag{16}$$

Simple chimney

$$X = 0; 0 < Y < D$$
$$U = V = 0; \Omega = -\frac{\partial^2 \Psi}{\partial X^2}\Big|_{X=0} \tag{17}$$
$$\frac{\partial \theta}{\partial X}\Big|_{X=0} = -(\tau_{gl}\alpha_{pv} - \eta_e)$$

$$X = 1; 0 < Y < D$$
$$U = V = 0; \Omega = -\frac{\partial^2 \Psi}{\partial X^2}\Big|_{X=1} \tag{18}$$
$$\frac{\partial \theta}{\partial X}\Big|_{X=1} = (\tau_{gl}\alpha_{abs}\alpha_{PV})$$

$$Y = 0; 0 < X < 1$$
$$U = 0; V = 1; \Psi = -X; \Omega = -\left.\frac{\partial^2 \Psi}{\partial X^2}\right|_{X=1}; \theta = 0 \qquad (19)$$

$$Y = 0; 0 < X < 1$$
$$U = V = 0; \Omega = -\left.\frac{\partial^2 \Psi}{\partial Y^2}\right|_{Y=0}; \left.\frac{\partial^2 \Psi}{\partial Y^2}\right|_{Y=0} = 0; \left.\frac{\partial \theta}{\partial Y}\right|_{Y=0} = 0 \qquad (20)$$

2.4 Assessment of heat transfer intensity

The transfer of heat through vertical walls subjected to heating may be described in terms of the Nuselt number, which represents a ratio of the conductive transfer of heat to the convective flux through the refrigerant. The following formula may calculate the local Nusselt number on the active plate with the photovoltaic (PV) cells at the coordinate $X=0$.

$$N_{uPV} = 1/\theta(Y) \qquad (21)$$

The electrical efficiency of a photovoltaic solar cell is expressed in the following way:

$$\eta_{el} = \eta_{ref} + \beta_{PV}(\overline{T_{PV}} - 298) + \gamma \log\left(\frac{\varphi}{1000}\right) \qquad (22)$$

The following relationship is used to evaluate the thermal efficiency of the chimney:

$$\eta_{th} = \frac{D_m C_f (T_0 - T_i)}{S_0 Q_0} \qquad (23)$$

$$\overline{T_{PV}} = \frac{1}{H} \int_0^H T_{PV}(y) dy \qquad (24)$$

$$D_m = \int_0^1 V(X, A) dx \qquad (25)$$

where, $\overline{T_{PV}}$ is the average temperature of the PV, T_0 is the temperature of the air leaving the chimney and T_i is the temperature of the air entering the chimney.

2.5 Numerical procedure

The implicit finite difference method was employed for the discretization of the heat and mass transfer equations associated with the solar chimney.

Approximations of the first and second derivatives of the diffusive terms were achieved through the use of central differences, while a second-order ascent scheme was employed for the convective terms to circumvent the potential instabilities inherent to mixed convection problems. The algebraic Eqs. (2) and (3) were integrated using the Thomas algorithm. In each iteration, the sequential points sub-relaxation method was employed to treat the Poisson equation, given by Eq. (4). The optimal sub-relaxation coefficient was found to be 0.8 for the grid with 51×101 points that were used in this study. At each time step, convergence of the iteration for the solution of the flow function is obtained. To ascertain the viability of a stable solution, the following criterion is employed. It is assumed that solutions will converge if the relative error for each variable between successive iterations is less than the convergence criterion ε. $\sum \left| \frac{\Phi^n(i,j) - \Phi^{n-1}(i,j)}{\Phi^n(i,j)} \right| \leq$

10^{-5}. Where Φ represents ψ, Θ, Ω; and n is the number of iterations. $\Delta\tau = 10^{-5}$ is the time step used in the calculations. The wall vorticity is approximated by the Woods formula. $\Omega_W = \frac{1}{2}\Omega_{W+1} - \frac{3}{\Delta\delta^2}(\Psi_{W+1} - \Psi_W)$, where Ψ_{W+1}, Ψ_W are the values of the stream function at the points adjacent to the boundary wall, δ is normal to the boundary wall. The data on the electrical and thermo-optical properties of the walls used in the calculations are shown in Table 1.

Table 1. Numerical model input characteristic values

Characteristic	Value
The absorption coefficient of the PV cell surface, α_pv	0.89 (-)
The transmittance of the PV cell surface, τ_pv	0.09 (-)
The reference temperature of the cells, T_{ref}	293 K
Reference temperature electrical efficiency, η_{ref}	0.015(-)
PV cell's temperature coefficient, β_{ref}	0.0045 K^{-1}

3. RESULTS AND DISCUSSION

3.1 Validation

To evaluate the computational code developed for this study, an investigation was conducted into the phenomenon of a vented cavity subjected to a constant heated flux emanating from its left vertical wall, while the remaining walls were considered to be insulated.

As evidenced in the study conducted by Raji et al. [22], there is a notable correlation between the solutions derived for the ventilated cavity and the results observed in the test case. Two apertures, situated in opposition to one another at the midpoint of the vertical plates and parallel to the horizontal walls, facilitate the entry and exit of fresh air into and out of the cavity when the system is introduced. All walls were subject to non-slip boundary conditions. For the Rayleigh number Ra fixed at 0, the Reynolds number Re was fixed at 100. The values of the current lines and the thermal fields in the ventilated cavity were predicted using numerical investigations. The results presented in Figure 2 are in perfect agreement with those reported in the study of Raji et al. [22].
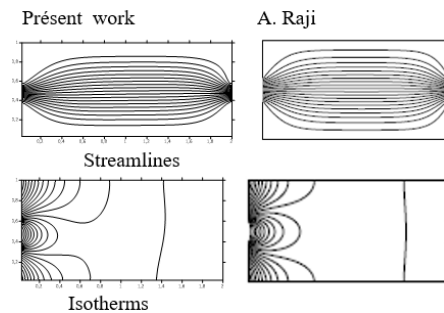

Figure 2. Validation of streamlines and isotherms

3.2 Dynamic and heat field visualisation

Figure 3 illustrates that the streamlines and temperature distribution of the structure follow the geometric relationship (B = H/d), with an aspect ratio of 8. The steady-state streamlines and isotherms for a fixed Rayleigh number (Ra) of 2.10^5 and Reynolds number of 100 are presented. The flow of air and the resulting distribution of temperatures (isotherms)

for the three types of chimneys (simple, combined, and shunt) are presented in Figures 3(a)-(c), respectively.
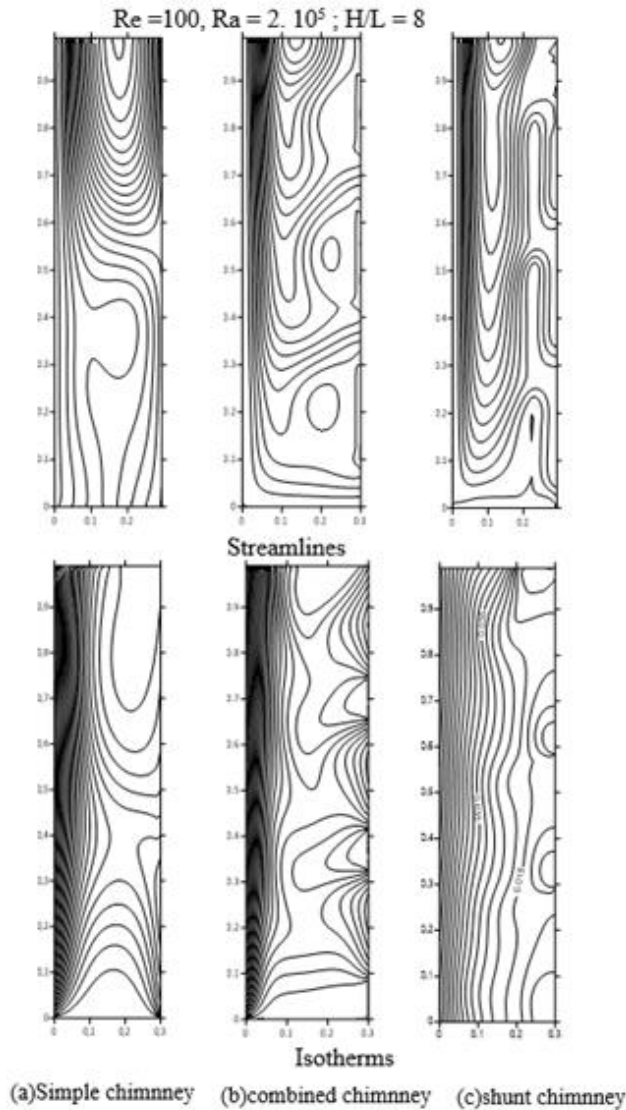

Figure 3. Visualization of streamlines and isotherms

The isotherms demonstrate the temperature variations, while the flow lines illustrate the adequate airflow through the ducts. It is evident that as heat transfer increases, isotherms narrow. The presence of both closed and open streamlines for return or recirculation flows indicates that mixed convection is the dominant mechanism in the stacks. As the heated air flows towards the chimney outlets, the airflow converges towards the PV cells, which are exposed to a constant heat flow. This evidence provides compelling support for the assertion that the optimal transfer method, mixed convection, is capable of extracting the maximum possible excess heat from the solar cells within the hybrid photovoltaic-thermal chimney. The isotherms for the three types of PV/T collector exhibit tight and nearly parallel profiles along the active wall surfaces. This suggests that heat transfer predominantly occurs via conduction near the photovoltaic panels. In the region situated at a distance from the active walls, the isotherms exhibit deformation and bifurcation, which indicates the occurrence of a convective heat transfer phenomenon.

A comparison of the Nusselt number (representing heat transfer intensity) for the primary chimney types is provided in Figure 4. The results demonstrate that the combined and

shunt stacks facilitate greater heat transfer than the single stacks. This improves the heat dissipation from the photovoltaic panels.
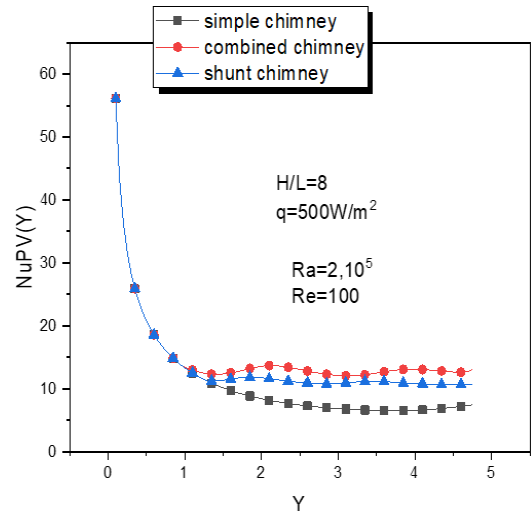

Figure 4. Variations of the local Nusselt number along the plate of solar stack PV cells
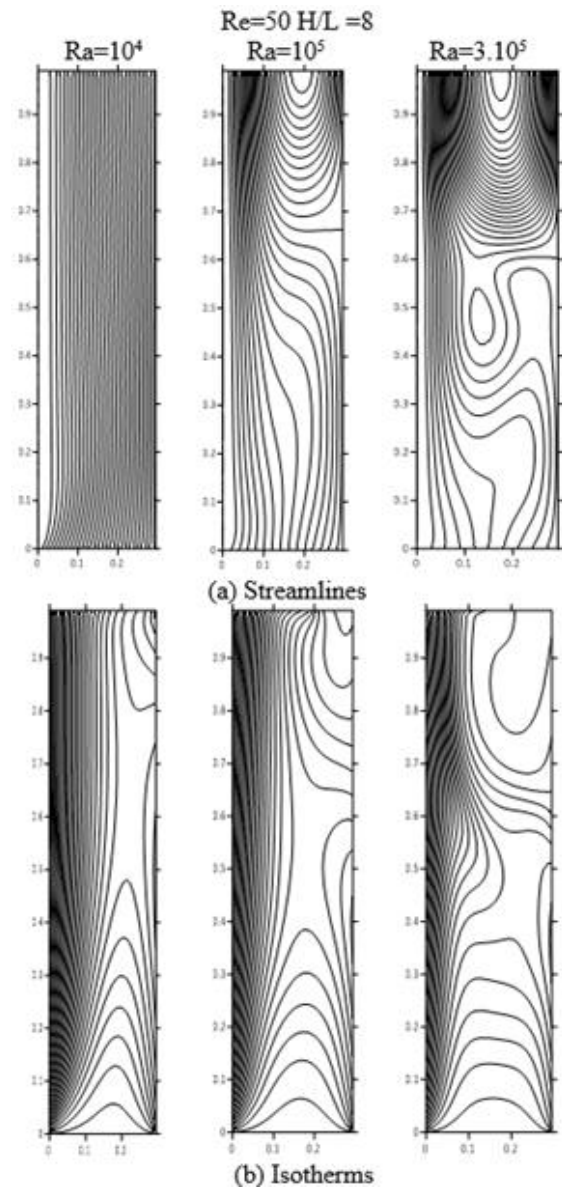

Figure 5. Variation of streamlines and isotherms in the simple chimney

3.3 Influence of the Rayleigh number of the chimney

Numerical analysis has been conducted to examine the effect of different Rayleigh numbers on airflow in solar chimneys. Figures 5(a), 6(a), and 7(a) illustrate the flow patterns and thermal fields within the chimneys, employing streamlines and isothermal contours. These figures illustrate how the airflow and thermal transfer within the stacks change with an increase in Rayleigh number. As the Rayleigh number increases, the volume of air flowing through the stacks rises, thereby enhancing the cooling of the PV panels, particularly in combined and shunted stacks. This configuration confers an advantage upon these novel chimneys, in that the PV cells are subjected to further cooling by the multiple openings of the fresh air jet inlet or the openings of the fresh air bypass channel. As illustrated in Figures 5(b), 6(b), and 7(b), there is an evident distortion of the isotherms as the Rayleigh number increases. This indicates that the majority of the heat transfer occurs within the solar cell area, as evidenced by the configuration of the isotherms in proximity to the PV cell panels or active walls. The isotherms display a high degree of parallelism. This suggests that the transfer of heat through the active walls is solely via conduction.
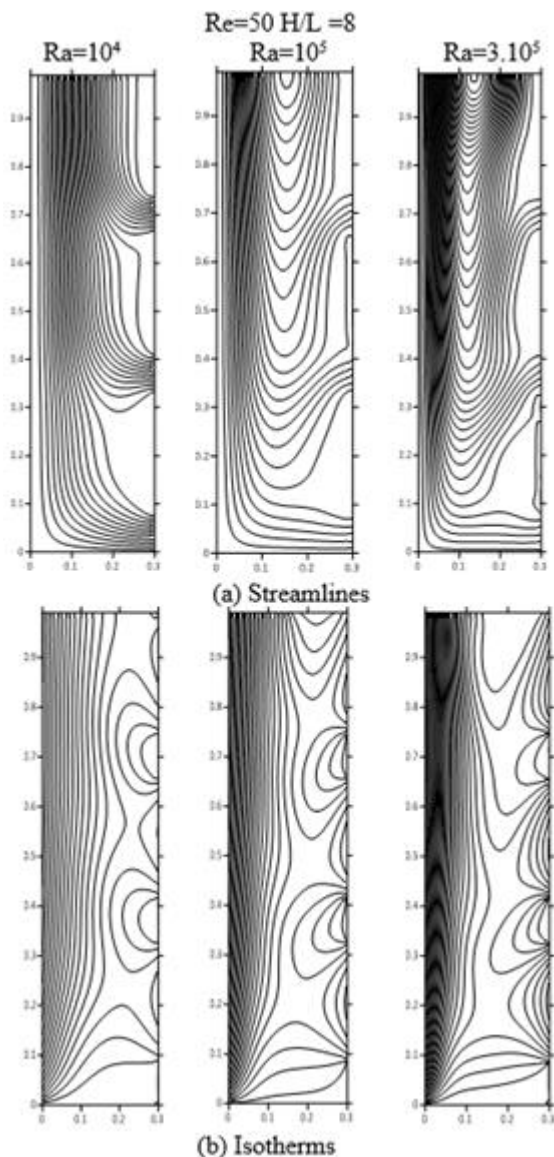
The local Nusselt number profiles as a function of the Rayleigh number, as about a single stack, a combined stack, and the stack in its entirety, are displayed in Figures 8, 9, and 10, respectively. The rate of heat transfer from the active walls to the heat transfer fluid is found to increase with the Rayleigh number. It can thus be stated that an increase in the Rayleigh number results in a corresponding increase in the local Nusselt number. These figures demonstrate that an increase in the Rayleigh number results in a corresponding increase in the Nusselt number, indicating that the transfer of heat from the PV panels to the fluids becomes more efficient as the airflow within the stacks rises. The variation of the local Nusselt number at the PV/T air collectors typically commences with a high value, which gradually decreases from a low value to an insignificant value towards the top, for all three categories of solar chimneys. Bilgen and Yamane [23] observed a comparable correlation between heat transfer and the Nusselt number, as a function of Rayleigh number, in their investigation of an enclosure with a chimney.
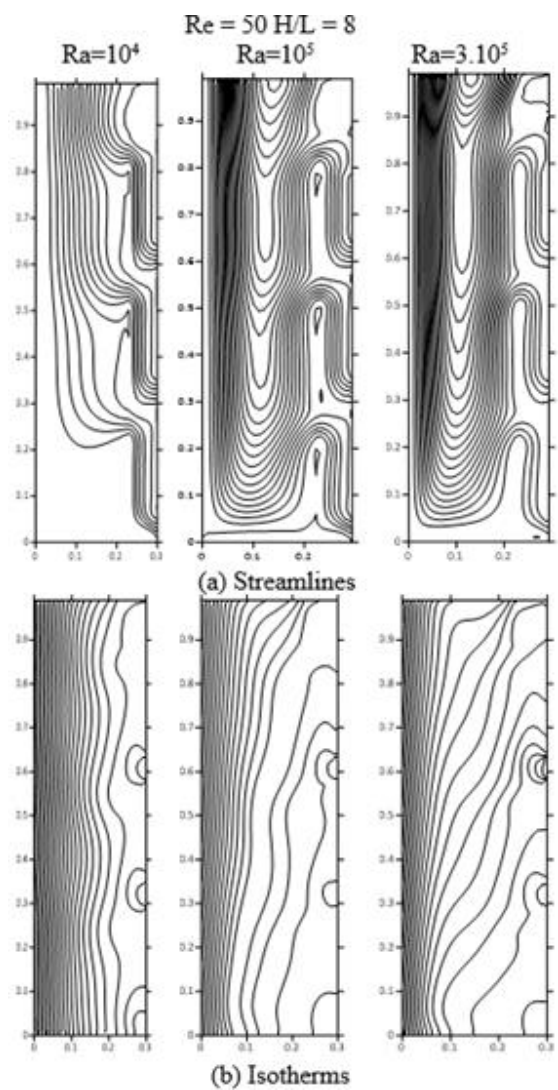

Figure 7. Variation of streamlines and isotherms in the shunt chimney

3.4 Electrical and thermal efficiencies of the chimneys

The results presented in Figure 11 illustrate a positive correlation between Reynolds number (Re) and thermal efficiency, indicating that increasing the Reynolds number enhances the recovery of heat from solar cells within

Figure 6. Variation of streamlines and isotherms in the combined chimney

chimneys. Figure 11 additionally illustrates that the shunt and combined chimneys exhibit superior thermal efficiency in comparison to a conventional chimney. Therefore, it can be concluded that both the shunt and combined chimney configurations offer superior mass draft airflow, as demonstrated in Figure 12. This enables the effective removal of excess heat from the back of the thermal photovoltaic (PV) panels. The results presented in Figure 13 demonstrate that for a reference efficiency of 15% of a crystalline silicon-based PV cell (ηref = 15%) [24], the combined or shunt chimneys equipped with three fresh air jet inlet openings, respectively, exhibit enhanced electrical efficiencies relative to that observed for the simple chimney with a single vertical air duct under identical conditions. This signifies that the period that the fresh air spends in the vertical duct is too brief, resulting in an insufficient dissipation of excess heat behind the thermal solar panel of the simple chimney. The maximum electrical efficiency of solar cells in combined or shunt chimneys with three fresh air jet inlet openings, respectively, is 14.7%; and 14.4% in comparison to 14% as shown in Figure 13, for solar cells in a solar chimney with a single vertical duct.
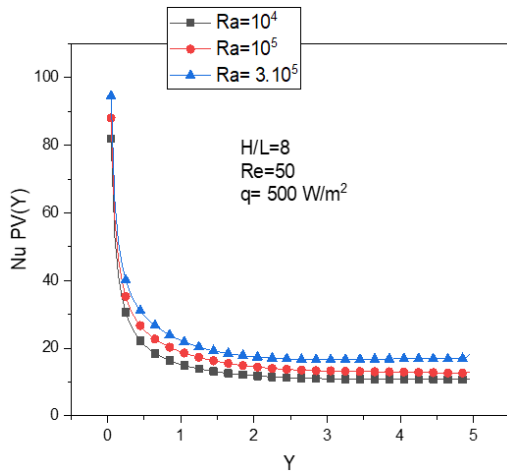

Figure 8. Variation of the local Nusselt number as a function of the Rayleigh number of the simple chimney
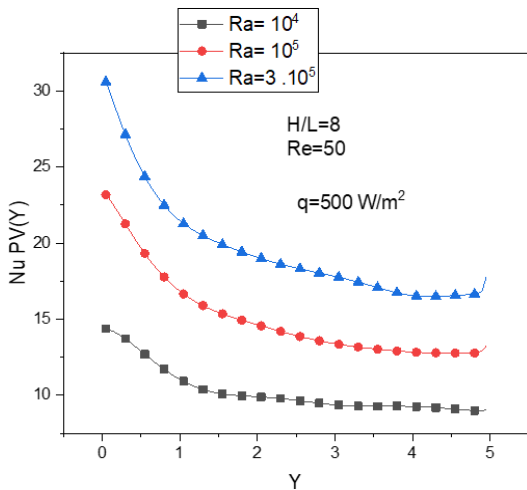

Figure 9. Variation of the local Nusselt number as a function of the Rayleigh number of the combined chimney

An improvement of 5% may be observed in terms of electrical efficiency. Similarly, the maximum thermal efficiency of solar cells in combined or shunt chimneys with three fresh air jet inlet openings is 67%, while that of solar cells in a solar chimney with a single vertical duct is 40%

(Figure 11). An improvement in thermal efficiency of 68% was observed. The aforementioned results align with those reported by other authors in the existing literature, who have demonstrated a correlation between elevated temperatures and reduced electrical efficiency in PV cells [25]. Consequently, the electrical efficiency of the cell plate exhibits a linear increase as a function of the Reynolds number, as illustrated in Figure 13.
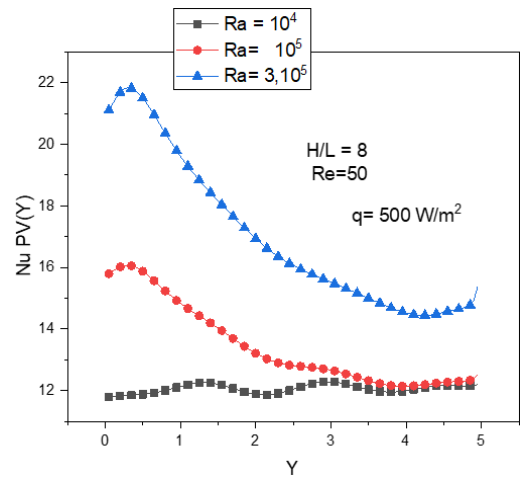

Figure 10. Variation of the local Nusselt number as a function of the Rayleigh number of the shunt chimney
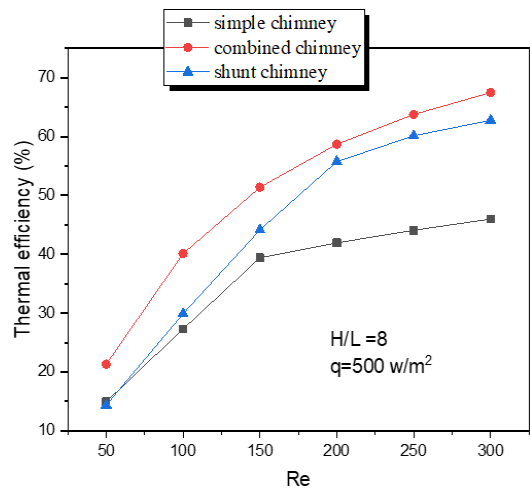

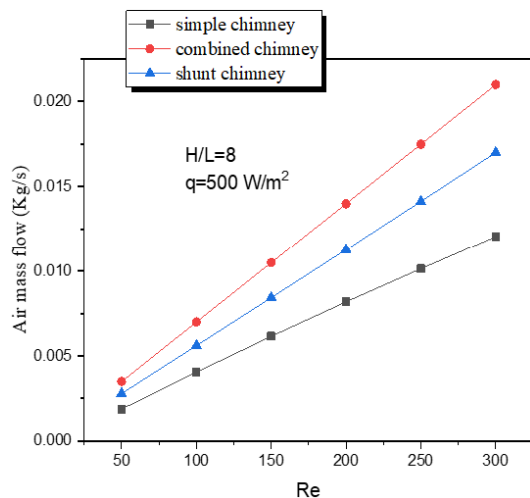**Figure 11.** Variation of Thermal efficiency versus the Reynolds number

Figure 12. Variation of the mass flow of air at the outlet of chimneys versus the Reynolds number
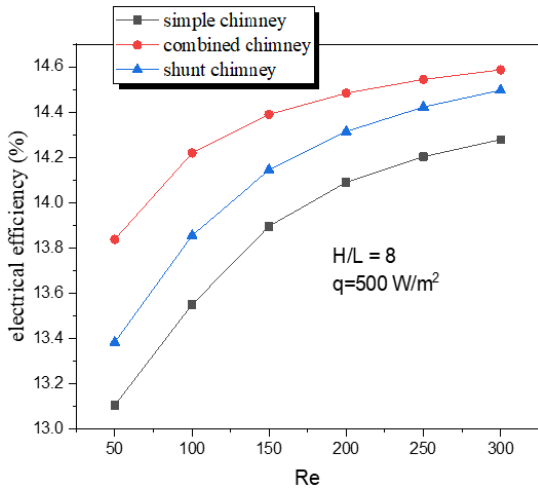
Figure 13. Variation of the electrical efficiency of PV cells in the chimneys versus the Reynolds number

3.5 Influence of the number of fresh air jet inlet openings

3.5.1 Combined chimney

The efficacy of a series of geometric air channel configurations, comprising two inlets, three inlets, four inlets, five inlets, and single inlets, is evaluated through a comparative assessment. The results are presented in terms of electrical, thermal, and mass flow efficiencies in Figures 14, 15, and 16. The data indicates that there is an increase in electrical and thermal efficiencies and mass flow rate with an increase in the number of openings in the fresh air jet inlets.
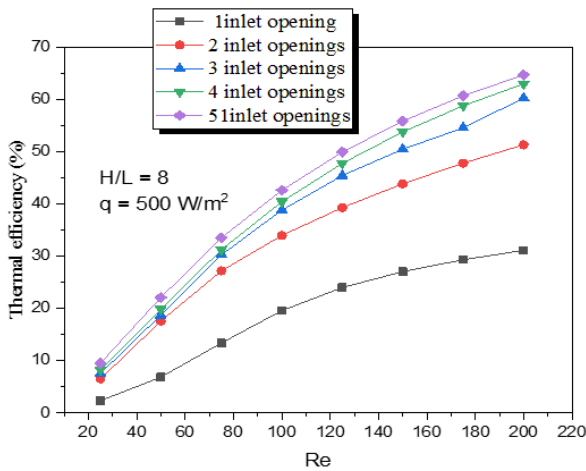

Figure 14. Influence of the number of fresh air inlet openings on thermal efficiency

Figure 14 illustrates that thermal efficiency increases in a linear fashion with the number of air inlet openings. For example, the use of five air inlets has been demonstrated to result in a thermal efficiency that is approximately twice as high as that achieved with a single inlet. This increase can be attributed to the enhanced disturbance of the air boundary layer on the surface of the photovoltaic panel, which in turn facilitates improved convective heat transfer. Furthermore, the electrical efficiency demonstrates a similar upward trend with the number of air inlets, as illustrated in Figure 15. Nevertheless, the variation is less pronounced than in the case of thermal efficiency. The reduction in temperature of the PV panels as a result of heat dissipation has a less pronounced impact on electrical efficiency. The air mass flow rate

demonstrates a notable increase in the number of air inlet openings, indicating that systems with multiple fresh air inlets facilitate enhanced air circulation, which contributes to superior heat dissipation (Figure 16).
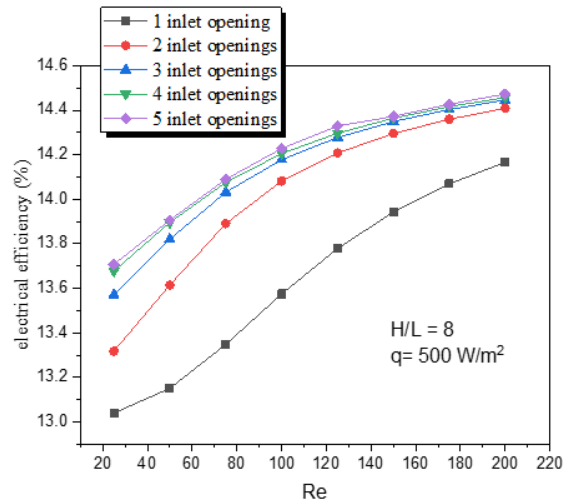

Figure 15. Influence of the number of fresh air jet inlet openings on electrical efficiency
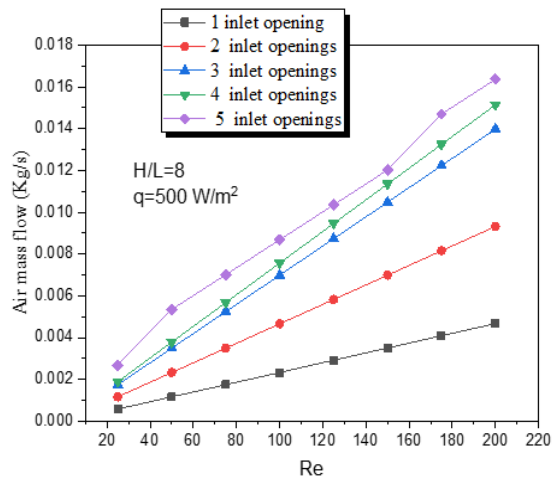

Figure 16. Influence of the number of fresh air jet inlet openings on the mass flow of air at the chimney outlet
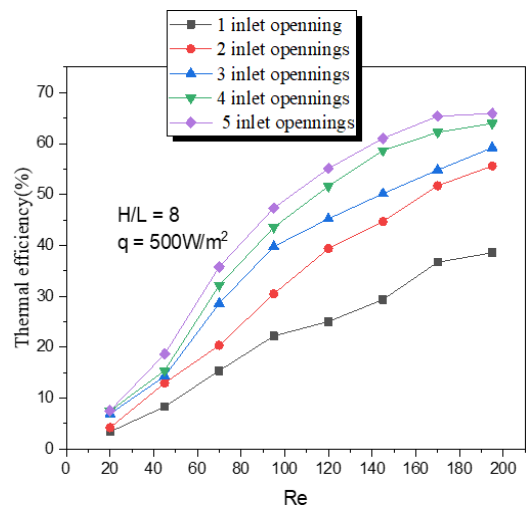

Figure 17. Influence of the number of fresh air jet inlet openings on the thermal efficiency of the shunt chimney
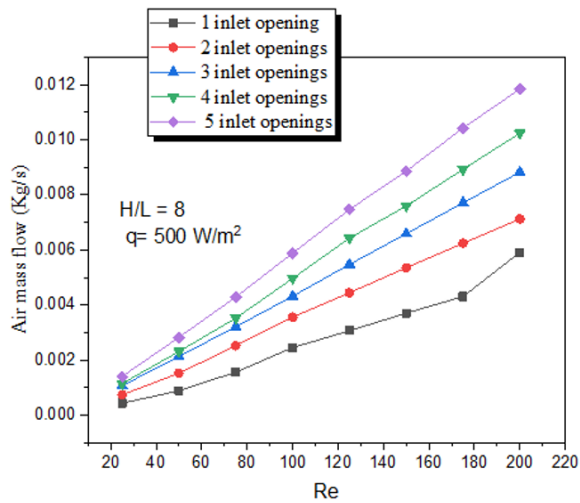
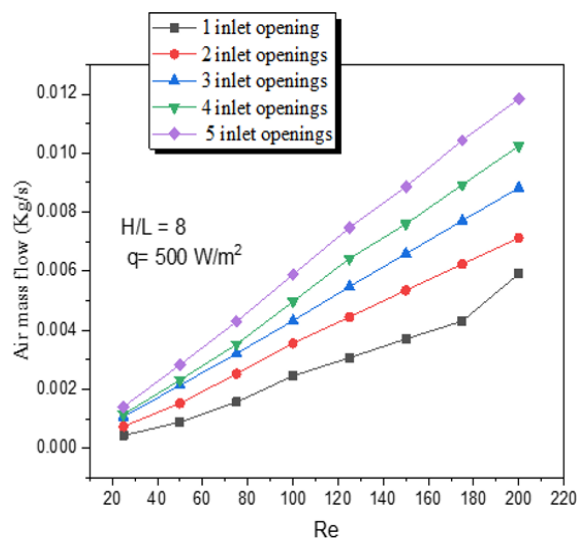**Figure 18.** Influence of the number of fresh air jet inlet openings on the mass flow rate for the shunt chimney

Figure 19. Influence of the number of fresh air jet inlet openings on the electrical efficiency of the chimney

3.5.2 Shunt chimney

The present study compares five distinct air channel configurations, comprising 2 inlets, 3 inlets, 4 inlets, 5 inlets, and a single inlet configuration. The results are displayed concerning thermal and electrical efficiency, as well as mass airflow at the outlet of the chimneys, as illustrated in Figures 17, 18, and 19. An increase in the number of apertures for the input of fresh air in the shunt chimney is accompanied by an increase in its thermal efficiency (Figure 17). The photovoltaic cells lose a greater quantity of heat when more apertures are created, which results in a reduction in temperature and an enhancement in heat recovery efficiency. The configuration comprising five intake apertures exhibits optimal thermal efficiency, representing a substantial enhancement over designs with a reduced number of openings. As evidenced in Figure 18, an increase in the number of fresh air jet inlet openings correlates with an increase in the mass flow rate at the outlet of the shunt chimney. This signifies that an augmented number of inlets facilitates the intake of a greater volume of air, thereby optimising the ventilation and heat removal capacity of the system. The greater the circulation of air within the chimney, the more effectively it will remove excess heat from the photovoltaic cells, thereby enhancing the

overall thermal performance. Furthermore, an increase in the number of inlet openings for the flow of fresh air results in enhanced electrical efficiency. The incorporation of supplementary inlets has been observed to engender a more efficacious cooling effect, which in turn serves to reduce the temperature of the photovoltaic cells and thereby enhance their performance. A reduction in the temperature of the solar cells results in an increase in electrical power, which in turn leads to an improvement in electrical efficiency.

4. CONCLUSIONS

The findings of this study demonstrate that the utilization of solar chimneys equipped with multiple fresh air inlets substantially enhances the thermal and electrical efficiency of photovoltaic/thermal (PV/T) systems. The thermal efficiency increased by 68% and the electrical efficiency by 5% in comparison to a single chimney, as a consequence of the enhanced dissipation of the heat generated by the photovoltaic panels. These findings substantiate the value of multiple ventilation in optimizing the performance of PV/T systems. The findings of this study are applicable to residential, commercial, and industrial solar integrated energy systems. The integration of solar chimneys with multiple air inlets facilitates the optimization of electricity production while simultaneously recovering heat for utilization in heating buildings or powering hot water systems. Such systems could prove invaluable in regions characterized by high temperatures, where the risk of overheating photovoltaic panels is a significant concern, as well as in installations that necessitate both electrical and thermal energy, including smart buildings and exo-energy infrastructure. The present study offers substantial insights into enhancing photovoltaic-thermal (PV/T) systems by employing solar chimneys with integrated fresh air inlets. Nevertheless, as with any research project, several limitations warrant acknowledgment. The aforementioned limitations also provide opportunities for further improvements and research in this area. The study's primary methodology is numerical modelling, utilizing techniques including implicit finite differences, the Gauss-Seidel scheme, and the Thomas algorithm. Although this approach is effective for controlled scenarios, it fails to take into account some dynamic aspects of the real behaviour of the systems, including weather variations and transient effects. The research is primarily concerned with thermal and electrical efficiency, but it does not consider the costs associated with installing chimneys with multiple fresh air intakes or the materials required to optimize heat transfer.

The subsequent phase of this research will involve the construction of a prototype experimental solar chimney comprising multiple fresh air inlets, to be subsequently tested in a controlled external environment. A further study in situ would enable the authors to validate the numerical results and evaluate the performance of the system in real conditions. Future studies could introduce simulations of turbulent flows in stacks to more accurately assess the performance in situations where laminar flow cannot be maintained.

REFERENCES

[1] Palanisamy, R., Vijayakumar, K., Bagchi, A., Gupta, V., Sinha, S. (2017). Implementation of coupled inductor

based 7-level inverter with reduced switches. International Journal of Power Electronics and Drive Systems, 8(3): 1294-1302. https://doi.org/10.11591/ijpeds.v8i3.pp1294-1302

[2] Fudholi, A., Sopian, K. (2018). Review on exergy and energy analysis of solar air heater. International Journal of Power Electronics and Drive Systems, 9(1): 420-426. https://doi.org/10.11591/ijpeds.v9.i1.pp420-426

[3] Fudholi, A., Sopian, K. (2018). R&D of Photovoltaic Thermal (PVT) Systems: an overview. International Journal of Power Electronics and Drive Systems, 9(2): 803-810. https://doi.org/10.11591/ijpeds.v9.i2.pp803-810

[4] Etier, I., Nijmeh, S., Shdiefat, M., Al-Obaidy, O. (2021). Experimentally evaluating electrical outputs of a PV-T system in Jordan. International Journal of Power Electronics and Drive Systems, 12(1): 421-430. https://doi.org/10.11591/ijpeds.v12.i1.pp421-430

[5] Salameh, T., Tawalbeh, M., Juaidi, A., Abdallah, R., Hamid, A.K. (2021). A novel three-dimensional numerical model for PV/T water system in hot climate region. Renewable Energy, 164: 1320-1333. https://doi.org/10.1016/j.renene.2020.10.137

[6] El Alami, Y., Lamkaddem, A., Bendaoud, R., Talbi, S., Baghaz, E. (2024). Numerical study of a water-based photovoltaic-thermal (PVT) hybrid solar collector with a new heat exchanger. e-Prime-Advances in Electrical Engineering, Electronics and Energy, 9: 100693. https://doi.org/10.1016/j.prime.2024.100693

[7] Xu, Z., Kleinstreuer, C. (2014). Concentration photovoltaic–thermal energy co-generation system using nanofluids for cooling and heating. Energy Conversion and Management, 87: 504-512. https://doi.org/10.1016/j.enconman.2014.07.047

[8] Sathyamurthy, R., Kabeel, A.E., Chamkha, A., Karthick, A., Muthu Manokar, A., Sumithra, M.G. (2021). Experimental investigation on cooling the photovoltaic panel using hybrid nanofluids. Applied Nanoscience, 11(2): 363-374. https://doi.org/10.1007/s13204-020-01598-2

[9] Aydın, A., Kayri, İ., Aydin, H. (2024). Electrical and thermal performance enhancement of a photovoltaic thermal hybrid system with a novel inner plate-finned collective cooling with different nanofluids. International Journal of Green Energy, 21(3): 555-569. https://doi.org/10.1080/15435075.2023.2201345

[10] Nijmeh, S., Yaseen, A.I.B., Juaidy, M. (2022). Numerical investigation of a solar PV/T air collector under the climatic conditions of Zarqa, Jordan. International Journal of Renewable Energy Development, 11(4): 963. https://doi.org/10.14710/ijred.2022.45306

[11] Slimani, M.E.A., Amirat, M., Kurucz, I., Bahria, S., Hamidat, A., Chaouch, W.B. (2017). A detailed thermal-electrical model of three photovoltaic/thermal (PV/T) hybrid air collectors and photovoltaic (PV) module: Comparative study under Algiers climatic conditions. Energy Conversion and Management, 133: 458-476. https://doi.org/10.1016/j.enconman.2016.10.066

[12] Dunne, N.A., Liu, P., Elbarghthi, A.F., Yang, Y., Dvorak, V., Wen, C. (2023). Performance evaluation of a solar photovoltaic-thermal (PV/T) air collector system. Energy Conversion and Management: X, 20: 100466. https://doi.org/10.1016/j.ecmx.2023.100466

[13] Patil, M., Sidramappa, A., Hebbale, A.M., Vishwanatha, J.S. (2023). Computational fluid dynamics (CFD) analysis of air-cooled solar photovoltaic (PV/T) panels. Materials Today: Proceedings. https://doi.org/10.1016/j.matpr.2023.05.198

[14] Sardarabadi, M., Passandideh-Fard, M., Heris, S.Z. (2014). Experimental investigation of the effects of silica/water nanofluid on PV/T (photovoltaic thermal units). Energy, 66: 264-272. https://doi.org/10.1016/j.energy.2014.01.102

[15] Choi, H.U., Choi, K.H. (2020). Performance evaluation of PV/T air collector having a single-pass double-flow air channel and non-uniform cross-section transverse rib. Energies, 13(9): 2203. https://doi.org/10.3390/en13092203

[16] Mojumder, J.C., Chong, W.T., Ong, H.C., Leong, K.Y. (2016). An experimental investigation on performance analysis of air type photovoltaic thermal collector system integrated with cooling fins design. Energy and Buildings, 130: 272-285. https://doi.org/10.1016/j.enbuild.2016.08.040

[17] Badi, N., Laatar, A.H. (2024). Improved cooling of photovoltaic panels by natural convection flow in a channel with adiabatic extensions. Plos one, 19(7): e0302326. https://doi.org/10.1371/journal.pone.0302326

[18] Chow, T.T., He, W., Ji, J. (2007). An experimental study of façade-integrated photovoltaic/water-heating system. Applied Thermal Engineering, 27(1): 37-45. https://doi.org/10.1016/j.applthermaleng.2006.05.015

[19] Xu, L., Luo, K., Ji, J., Yu, B., Li, Z., Huang, S. (2020). Study of a hybrid BIPV/T solar wall system. Energy, 193: 116578. https://doi.org/10.1016/j.energy.2019.116578

[20] Chen, Y., Athienitis, A.K., Galal, K. (2010). Modeling, design and thermal performance of a BIPV/T system thermally coupled with a ventilated concrete slab in a low energy solar house: Part 1, BIPV/T system and house energy concept. Solar Energy, 84(11): 1892-1907. https://doi.org/10.1016/j.solener.2010.06.013

[21] Lukasik, J., Wajs, J. (2024). Experimental and numerical study of thermal and electrical potential of BIPV/T collector in the form of air-cooled photovoltaic roof tile. International Journal of Heat and Mass Transfer, 227: 125554. https://doi.org/10.1016/j.ijheatmasstransfer.2024.125554

[22] Raji, A., Hasnaoui, M., Bahlaoui, A. (2008). Numerical study of natural convection dominated heat transfer in a ventilated cavity: Case of forced flow playing simultaneous assisting and opposing roles. International Journal of Heat and Fluid Flow, 29(4): 1174-1181. https://doi.org/10.1016/j.ijheatfluidflow.2008.01.010

[23] Bilgen, E., Yamane, T. (2004). Conjugate heat transfer in enclosures with openings for ventilation. Heat and Mass Transfer, 40: 401-411. https://doi.org/10.1007/s00231-003-0418-z

[24] Mittelman, G., Alshare, A., Davidson, J.H. (2009). A model and heat transfer correlation for rooftop integrated photovoltaics with a passive air cooling channel. Solar Energy, 83(8): 1150-1160. https://doi.org/10.1016/j.solener.2009.01.015

[25] Skoplaki, E., Palyvos, J.A. (2009). On the temperature dependence of photovoltaic module electrical performance: A review of efficiency/power correlations.

NOMENCLATURE

c_p	Calorific capacity (J. Kg^{-1}. °C^{-1})
d	Chimney width (m)
g	Acceleration of gravity (m.s^{-2})
h	Convective Transfer Coefficient (W m^{-2}K^{-1})
H	Overall height of the chimney(m)
D	The ratio of total height to the width of the chimney
S	The ratio of the height of the second level to the width of the chimney
W	Wall
A	The ratio of the height of the first level to the width of the chimney
T	The ratio of the first entrance to the width of the chimney
K	The ratio of the height of the third level to the width of the chimney
P	The ratio of the height of the second level to the width of the chimney
L	Total length of the room (m)
Gr	Grashof number (-)
Pr	Prandtl number (-)
Re	Reynolds number (-)
t	Time (s)

T	Temperature (K)
T_a	Ambient air temperature (K)
T_M	Material Temperature (K)
u, v	Components of directional velocity x et y (m.s^{-1})
U, V	Dimensionless components of speed in directions X et Y, $U = u/u_0$, $V = v/u_0$, (-)
u_0	Air inlet velocity in the chimney (m.s^{-1})
X, Y	Dimensionless Cartesian coordinates (-)
x, y	Cartesian coordinates (m)

Greek letters

Ω	Dimensionless vorticity (-)
ω	Dimensional vorticity (s^{-1})
ψ	Dimensional Current Function (m^2.s^{-1})
Ψ	Dimensionless current function (-)
Θ	Dimensionless Temperature (-)
τ	Dimensionless Time (-)
λ	Coefficient of Thermal Conductivity (W.m^{-1}.°C^{-1})
μ	Dynamic Viscosity of Air (Kg.m^{-1}.s^{-1})
ρ	Air density (Kg.m^{-3})
τ	Transmission coefficient
η_{el}	Electrical efficiency of cells PV (-)
η_{th}	Thermal efficiency of the chimney (-)
Φ	The density of solar flux (W.m^{-2})